CHAPTER 4 Results and Discussion

4.1 Fourier Transform Infrared Spectroscopy

4.1.1 Copper(II) 4–Aminobenzoate

Copper(II) 4-aminobenzoate (CAB) was prepared from 4-aminobenzoic acid and copper(II) acetate monohydrate. Fourier Transform Infrared (FTIR) spectra of the materials are shown in Figure 4.1- 4.3 and the data collected in Table 4.1.

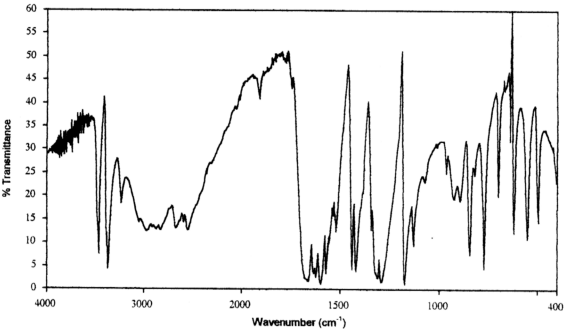

Figure 4.1 FTIR spectrum of 4-aminobenzoic acid

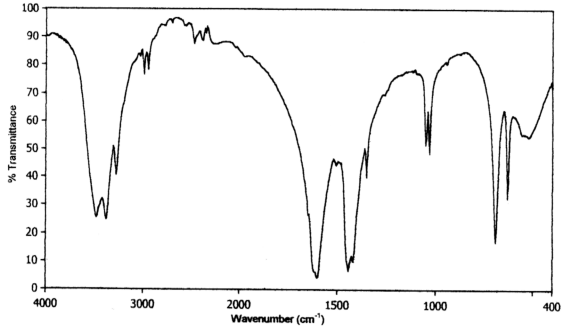

Figure 4.2 FTIR spectrum of copper(II) acetate monohydrate

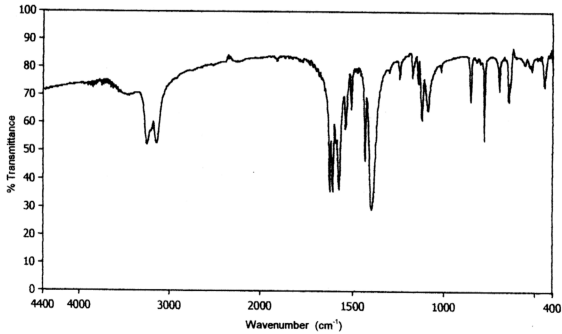

Figure 4.3 FTIR spectrum of copper(II) 4-aminobenzoate

Table 4.1 FTIR data of 4-aminobenzoic acid, copper(II) acetate monohydrate and copper(II) 4-aminobenzoate

Assignment	Wavenumbers/cm^{-1}		
	4-Aminobenzoic acid	Copper(II) acetate monohydrate	Copper(II) 4-aminobenzoate
C-H (aromatic) Asymmetrical stretching	3230 (w)	—	3474 (s)
N-H Asymmetrical stretching	3460 (s, sh)	—	3255 (m)
N-H Symmetrical stretching	3363 (s, sh)	—	3142 (m)
-OH	3000-2500 (m, br)	3474-3271 (s, br)	—
C-H (aliphatic) Stretching	—	2941 (w)	—
-COO Asymmetrical stretching	1668 (s, br)	1601 (s)	1609 (m)
-COO Symmetrical stretching	1442 (s)	1445 (s)	1434 (m)
$-CH_3$ Asymmetrical bending	—	1601 (s)	—
$-CH_3$ Symmetrical bending	—	1445 (s)	—
C=C (aromatic) Asymmetrical stretching	1623 (s, sh)	—	1625 (s)
C=C (aromatic) Symmetrical stretching	1423 (s, sh)	—	1397 (s)
C-N Stretching	1312 (s)	—	1397 (s)
N-H Wagging	852 (s)	—	853 (m)
Para substituted aromatic ring	771 (s)	—	778 (m)

s, strong ; m, medium ; w, weak ; br, broad ; sh, sharp

The results indicate that the spectrum of CAB (Figure 4.3) is distinctly different from that of its starting materials (Figure 4.1 and 4.2), confirming that a reaction has occurred between 4-aminobenzoic acid and copper(II) acetate monohydrate to form copper(II) 4-aminobenzoate, as written in chemical equation shown below

$$Cu[CH_3COO]_2 + 2\ C_6H_4(NH_2)COOH \xrightarrow{\text{Acetonitrile}} Cu[C_6H_4NH_2COO]_2 + 2CH_3COOH$$

The spectrum of CAB (Figure 4.3) showed bands due to the presence of functional groups and bonds expected of it, namely N-H at 3255 cm^{-1} and 3142 cm^{-1}, aromatic C-H at 3474 cm^{-1}, COO (bidentate, bridging) at 1609 cm^{-1} and 1434 cm^{-1} [1], aromatic C=C at 1625cm^{-1} and 1397 cm^{-1} and para-substituted aromatic ring at 778 cm^{-1}. From these findings and with reference to the structure of copper(II) acetate [2], a proposed structure of CAB is shown in Figure 4.4.

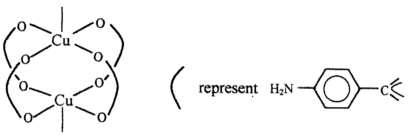

Figure 4.4 Proposed structure of copper(II) 4-aminobenzoate

Several interesting conclusions may be made when the wavenumbers of functional groups and bonds of CAB are further analysed. Firstly, the N-H bands in CAB at 3255 cm^{-1} and 3142 cm^{-1} are at lower wavenumbers compared to that of 4-aminobenzoic acid (at 3460 $cm^{-1}$and 3363 cm^{-1}). Secondly, the C-N bond for CAB (at 1397 cm^{-1}) is at higher wavenumber compared to that of 4-aminobenzoic acid (at 1312 cm^{-1}). Thirdly, the -COO bands in CAB (at 1609 cm^{-1} and 1434 cm^{-1}) are at lower wavenumbers compared to that of 4-aminobenzoic acid (at 1668 cm^{-1} and 1442 cm^{-1}). The shift in the wavenumbers for these functional groups and bonds indicate that 4-aminobenzoate ligand undergo resonance as shown in Figure 4.5.

Figure 4.5 Resonance in 4-aminobenzoate ligand

The resonance which occurs weaken the N-H bond but strengthen the C-N bond, because of the partial double bond formed. It also increases conjugation by destroying aromaticity in the ring and causes electron drift towards copper(II) ions. The positive charge developed on nitrogen may hinder the formation of H-bonds between CAB chains.

4.1.2 Copper(II) 4–Aminobenzoate Doped with Iodine

Copper(II) 4-aminobenzoate (CAB) was doped with different amounts of iodine (4% to 28%). The FTIR spectra of the doped samples were shown in Figure 4.6 and the data collected in Table 4.2. The spectrum and data for undoped CAB were also included for comparison.

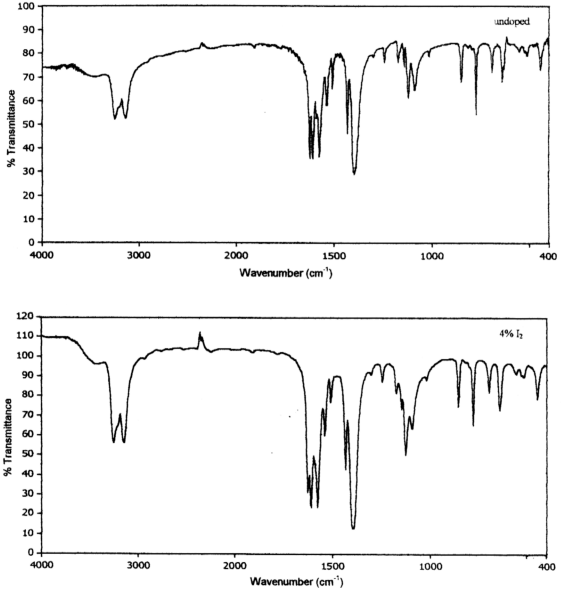

Figure 4.6 FTIR spectra of copper(II) 4-aminobenzoate doped with different amounts of iodine

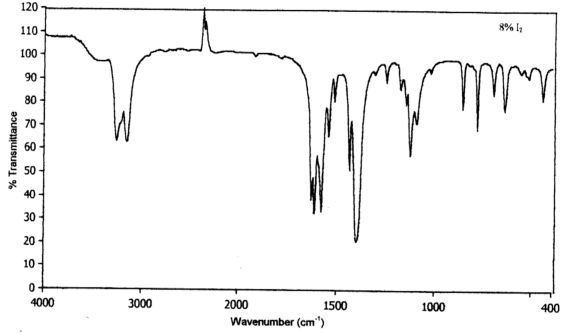

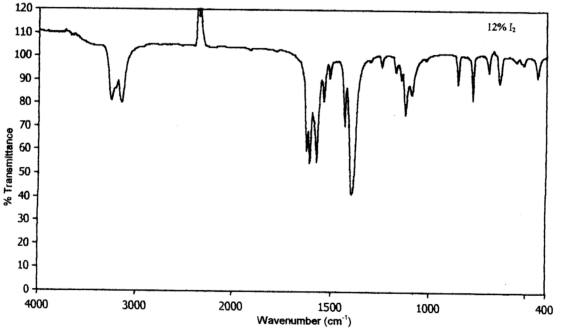

Figure 4.6 FTIR spectra of copper(II) 4-aminobenzoate doped with different amounts of iodine (continue)

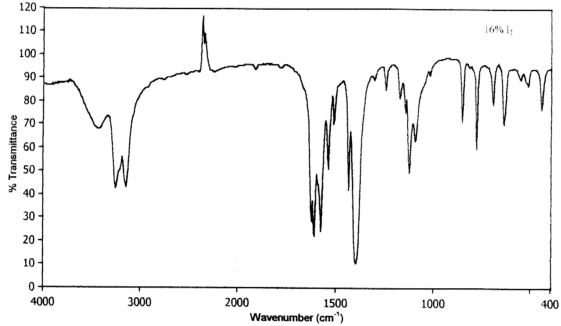

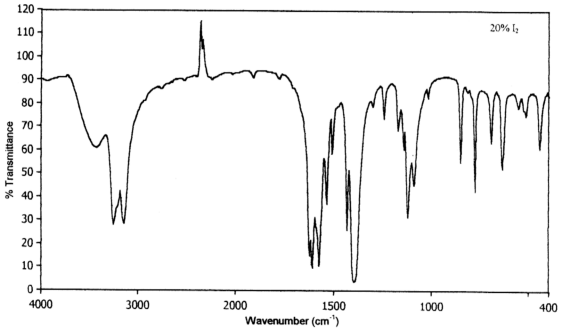

Figure 4.6 FTIR spectra of copper(II) 4-aminobenzoate doped with different amounts of iodine (continue)

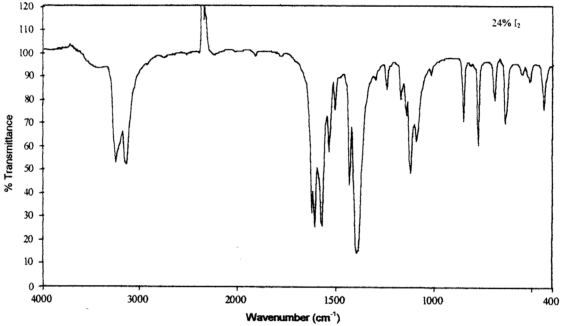

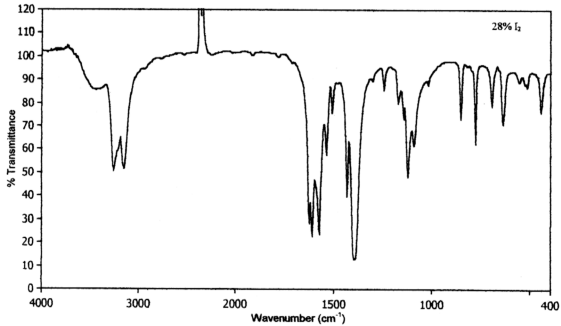

Figure 4.6 FTIR spectra of copper(II) 4-aminobenzoate doped with different amounts of iodine (continue)

Table 4.2 FTIR data (in cm^{-1}) for copper(II) 4-aminobenzoate doped with different amounts of iodine

Assignment	% Iodine							
	0	4	8	12	16	20	24	28
C-H (aromatic) Asymmetrical stretching	3474 (w)	3435 (w)	3446 (w)	3452 (w)	3435 (m)	3435 (m)	3457 (w)	3457 (m)
N-H Asymmetrical stretching	3255 (m)	3252 (m)	3253 (m)	3254 (m)	3253 (m)	3253 (m)	3253 (m)	3253 (m)
N-H Symmetrical stretching	3142 (m)	3142 (m)	3143 (m)	3143 (m)	3142 (m)	3143 (m)	3143 (m)	3143 (m)
-COO bidentate, bridging Asymmetrical stretching	1609 (m)	1608 (m)	1609 (m)	1609 (m)	1610 (m)	1610 (m)	1609 (m)	1609 (m)
-COO bidentate, bridging Symmetrical stretching	1434 (m)	1434 (m)	1434 (m)	1434 (m)	1434 (m)	1434 (m)	1434 (m)	1434 (m)
C=C (aromatic) Asymmetrical stretching	1625 (s)	1624 (s)	1625 (s)	1625 (s)	1624 (s)	1625 (s)	1625 (s)	1625 (s)
C=C (aromatic) Symmetrical stretching C-N Stretching	1397 (s)	1396 (s)	1397 (s)	1398 (s)	1398 (s)	1398 (s)	1398 (s)	1397 (s)
N-H wagging	853 (m)	854 (m)	853 (m)	853 (m)	854 (m)	853 (m)	853 (m)	854 (m)
Para substituted of aromatic ring	778 (m)	778 (m)	778 (m)	778 (m)	778 (m)	778 (m)	778 (m)	778 (m)

s, strong ; m, medium ; w, weak ; br, broad

The results indicate that iodine, at these concentration range, did not affect the structure of CAB significantly. Iodine is a relatively weak oxidizing agent. It was used as dopant to effect the removal of electron(s) from CAB to form radial cation (CAB^+) and triiodide (I_3^-) and/or pentaiodide (I_5^-) counterion via complex formation [3]. The chemical equations are as follows.

$$CAB + I_2 \rightarrow (CAB)I_2$$

$$(CAB)I_2 \rightarrow [(CAB)I]^+ + I^-$$

$$[(CAB)I]^+ + (CAB)I_2 \rightarrow I_3^- + 2CAB^+$$

CAB radical cation is expected to retain all the functional groups and bonds present in CAB, and its structure is not expected to be much perturbed by the planar I_3^- counterion.

4.1.3 The Effect of Annealing on the Structure of Copper(II) 4–Aminobenzoate

Copper(II) 4-aminobenzoate (CAB) were annealed at 50^0C – 200^0C in nitrogen gas for 30 minutes. The FTIR spectra of the annealed samples were shown in Figure 4.7 and the data collected in Table 4.3. The spectrum and data for unannealed CAB were also included for comparison.

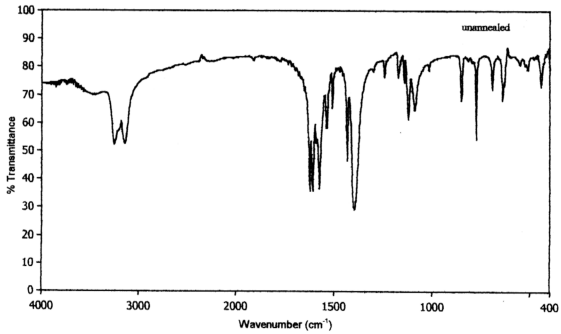

Figure 4.7 FTIR spectra of copper(II) 4-aminobenzoate annealed at different temperatures for 30 minutes (continue).

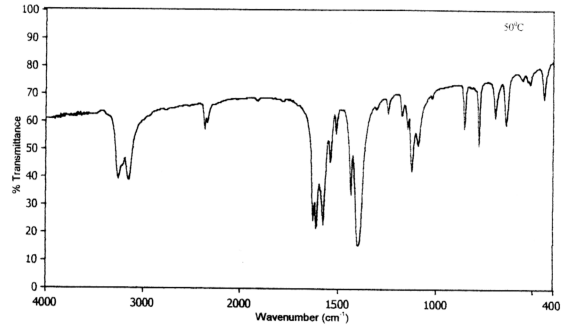

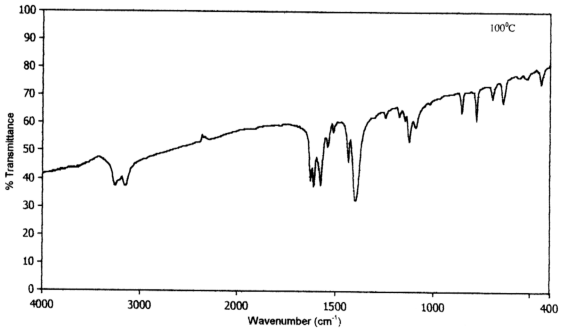

Figure 4.7 FTIR spectra of copper(II) 4-aminobenzoate annealed at different temperatures for 30 minutes (continue)

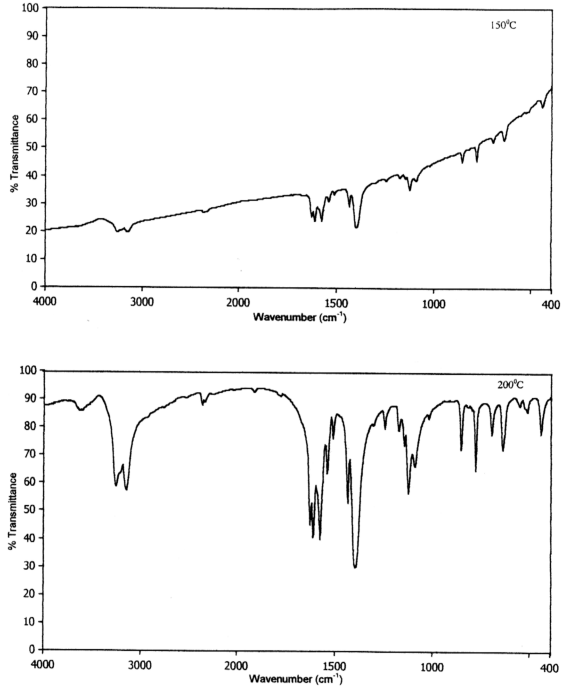

Figure 4.7 FTIR spectra of copper(II) 4-aminobenzoate annealed at different temperatures for 30 minutes (continue)

Table 4.3 FTIR data of copper(II) 4-aminobenzoate annealed at different temperatures for 30 minutes

Assignment	Annealed temperature (^{0}C)				
	unannealed	50	100	150	200
C-H (aromatic) Asymmetrical stretching	3474 (w)	3435 (w)	3446 (w)	3452 (w)	3435 (m)
N-H Asymmetrical stretching	3255 (m)	3252 (m)	3253 (m)	3254 (m)	3253 (m)
N-H Symmetrical stretching	3142 (m)	3142 (m)	3143 (m)	3143 (m)	3142 (m)
-COO bidentate, bridging Asymmetrical stretching	1609 (m)	1608 (m)	1609 (m)	1609 (m)	1610 (m)
-COO bidentate, bridging Symmetrical stretching	1434 (m)	1434 (m)	1434 (m)	1434 (m)	1434 (m)
C=C (aromatic) Asymmetrical stretching	1625 (s)	1624 (s)	1625 (s)	1625 (s)	1624 (s)
C=C (aromatic) Symmetrical stretching C-N stretching	1397 (s)	1396 (s)	1397 (s)	1398 (s)	1398 (s)
N-H wagging	853 (m)	854 (m)	853 (m)	853 (m)	854 (m)
Para substituted aromatic ring	778 (m)	778 (m)	778 (m)	778 (m)	778 (m)

s, strong ; m, medium ; w, weak ; br, broad

The results indicate that the structure of CAB was not perturbed at 50^{0}C but the material undergoes a transformation at 100^{0}C and 150^{0}C, and then return to its initial structure at 200^{0}C. It is noted that the functional groups and bonds are still present at these temperatures. The observations suggest that CAB oligomers cross-linked at 100-150^{0}C and the process was completed at 200^{0}C. Similar observation was noted for poly(p-phenylene vinylene) when heated in vacuum at 200^{0}C for 4 hours [4].

4.1.4 The Effect of Annealing on the Structure of Copper(II) 4-Aminobenzoate Doped with 20% Iodine

Copper(II) 4-aminobenzoate (CAB) doped with 20% iodine were annealed at 50^0C-200^0C in nitrogen gas for 30 minutes. The FTIR spectra of the annealed samples were shown in Figure 4.8 and the data collected in Table 4.4. The spectrum and data for unannealed CAB doped with 20% iodine were also included for comparison.

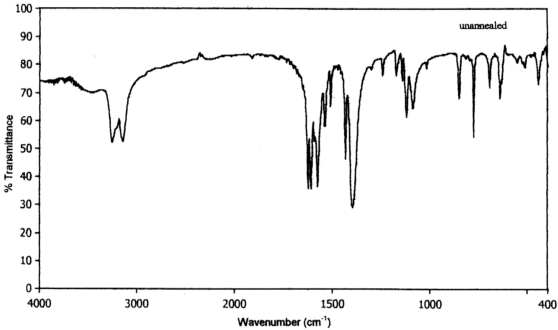

Figure 4.8 FTIR spectra of copper(II) 4-aminobenzoate doped with 20% iodine annealed at different temperatures for 30 minutes

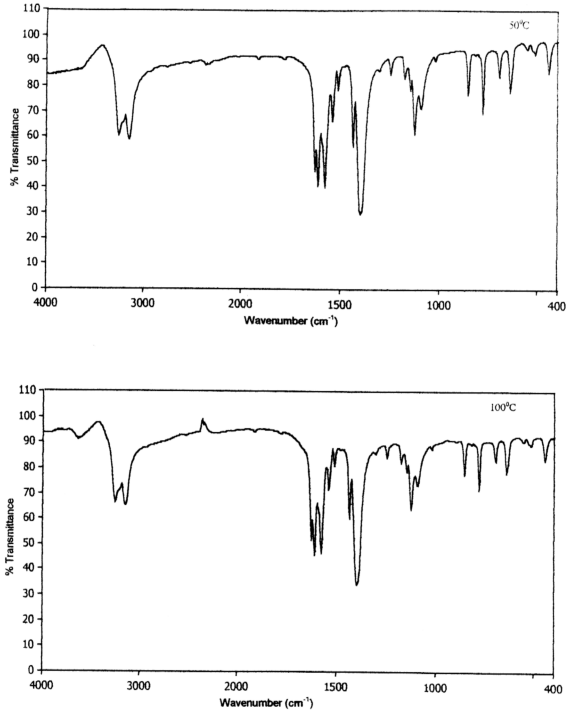

Figure 4.8 FTIR spectra of copper(II) 4-aminobenzoate doped with 20% iodine annealed at different temperatures for 30 minutes (continue)

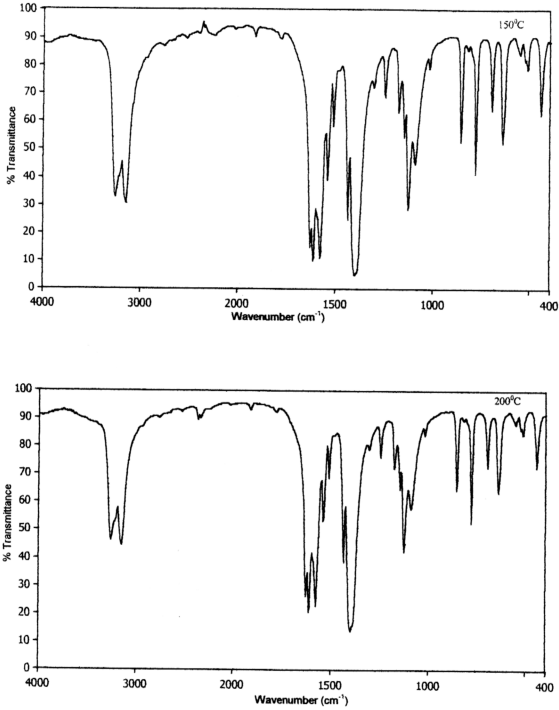

Figure 4.8 FTIR spectra of copper(II) 4-aminobenzoate doped with 20% iodine annealed at different temperatures for 30 minutes (continue)

Table 4.4 FTIR data (in cm^{-1}) for copper(II) 4-aminobenzoate doped with 20% iodine annealed at different temperature for 30 minutes

Assignment	Annealed temperature (^0C)				
	unannealed	50	100	150	200
C-H (aromatic) Asymmetrical stretching	3474 (w)	3435 (w)	3446 (w)	3452 (w)	3435 (m)
N-H Asymmetrical Stretching	3255 (m)	3252 (m)	3253 (m)	3254 (m)	3253 (m)
N-H Symmetrical stretching	3142 (m)	3142 (m)	3143 (m)	3143 (m)	3142 (m)
-COO bidentate, bridging Asymmetrical stretching	1609 (m)	1608 (m)	1609 (m)	1609 (m)	1610 (m)
-COO bidentate, bridging Symmetrical stretching	1434 (m)	1434 (m)	1434 (m)	1434 (m)	1434 (m)
C=C (aromatic) Asymmetrical stretching	1625 (s)	1624 (s)	1625 (s)	1625 (s)	1624 (s)
C=C (aromatic) Symmetrical stretching C-N stretching	1397 (s)	1396 (s)	1397 (s)	1398 (s)	1398 (s)
N-H wagging	853 (m)	854 (m)	853 (m)	853 (m)	854 (m)
Para substituted aromatic ring	778 (m)	778 (m)	778 (m)	778 (m)	778 (m)

s, strong ; m, medium ; w, weak ; br, broad

The results indicate that the structure of iodine-doped CAB was not perturbed at these temperature range, in contrast to that of undoped CAB under similar conditions. Iodine was suggested to effect the formation of CAB radical cations. These positively charged radicals would repel each other, thus inhibiting cross-linking.

4.1.5 Conclusion

FTIR spectroscopy confirmed the presence of all the functional groups and bonds expected to be present in CAB. It also indicated that 4-aminobenzoate ligand exist as resonance-stabilised bidentate bridging ligand. The structure of CAB is simple and there is little evidence of H-bonding involving the $-NH_2$ group presents at the para- position of the aromatic ring.

FTIR spectroscopy also indicated that the structure of CAB was not affected by iodine, and that the materials cross-linked at 100-150^{0}C but cross-linking did not occur when 20% iodine was present in the material.

4.2 Conductivity

The thickness of the disc, ℓ is measured using a digital vernier (Table 4.5). The diameter, d of the electrode is measured using a travelling microscope and the area of the electrode, A (Table 4.6) is calculated using the Equation 4.1

$$A = \pi \left(\frac{\bar{d}}{2} \right)^2 \qquad 4.1$$

where $\bar{d}$ is the average diameter.

Table 4.5 Thickness of sample

Percentage of Iodine (%)	Thickness ($\ell \pm 0.01$)mm										
	1	2	3	4	5	6	7	8	9	10	Average $\bar{\ell} \pm 0.01$
0.0	0.80	0.80	0.80	0.79	0.81	0.80	0.80	0.79	0.80	0.80	0.80
4.0	0.64	0.65	0.66	0.63	0.63	0.62	0.63	0.63	0.63	0.63	0.64
7.9	0.60	0.59	0.61	0.60	0.60	0.59	0.61	0.60	0.60	0.59	0.60
12.0	0.60	0.58	0.57	0.58	0.57	0.57	0.57	0.57	0.57	0.57	0.58
16.0	0.50	0.51	0.51	0.52	0.52	0.51	0.52	0.52	0.52	0.52	0.52
20.1	0.70	0.73	0.72	0.71	0.72	0.72	0.72	0.72	0.74	0.73	0.72
23.9	0.52	0.54	0.51	0.55	0.52	0.52	0.52	0.52	0.52	0.52	0.52
27.9	0.56	0.56	0.56	0.56	0.56	0.56	0.57	0.56	0.56	0.56	0.56

Table 4.6 Diameter of electrode

Percentage of Iodine (%)	Electrode Diameter (d ± 0.01)mm										Area (A ± 0.1) x10^{-4}m^2
	1	2	3	4	5	6	7	8	9	10	Average $\bar{d}$ /mm
0.0	2.60	2.48	2.64	2.40	2.55	2.41	2.48	2.53	2.57	2.51	2.51	5.0
4.0	2.10	1.92	2.23	2.02	1.96	2.04	2.18	1.99	2.22	2.00	2.07	3.4
7.9	2.10	2.23	1.91	2.20	1.96	2.14	2.09	2.01	1.99	2.08	2.07	3.4
12.0	2.40	2.26	2.30	2.31	2.32	2.39	2.36	2.29	2.33	2.34	2.33	4.3
16.0	1.90	1.97	1.98	2.13	1.96	1.89	2.07	2.03	1.99	2.01	1.99	3.1
20.1	2.20	2.36	2.26	2.40	2.13	2.19	2.24	2.16	2.15	2.25	2.23	3.9
23.9	3.48	3.25	3.29	3.50	3.27	3.50	3.19	3.11	3.20	3.31	3.31	8.6
27.9	2.30	2.32	2.21	2.64	2.48	2.33	2.29	2.30	2.36	2.35	2.36	4.4

An ohmic material obeys Ohm's law,

$$I = \frac{V}{R} \qquad 4.2$$

where, I, V and R are the current, potential difference and resistance respectively.

The conductivity, σ is calculated using the equation

$$\sigma = \frac{\bar{\ell}}{RA} \qquad 4.3$$

where $\bar{\ell}$ is the average thickness of the disc.

By substituting Equation 4.2 into Equation 4.3, the conductivity can be written as

$$\sigma = \frac{\bar{\ell} I}{AV} = \frac{\bar{\ell}}{A} m \qquad 4.4$$

where m is the gradient of the graph of I versus V in the ohmic region.

Taking the logarithm of Equation 4.2,

$$\log I = \log V - \log R \qquad 4.5$$

The ohmic region is where the gradient of graph log I versus log V equals to 1.

4.2.1 Conductivity of Copper(II) 4–Aminobenzoate

Figure 4.9 shows graphs of I versus V and log I versus log V for copper(II) 4–aminobenzoate (CAB) that obeys Ohm's law. The conductivity calculated for CAB is in the range 4.1-4.6x10^{-11} Scm^{-1} (Table 4.7). By comparison, the conductivity of copper(II) benzoate (CB) is 6.8x10^{-11} Scm^{-1} [5].

Table 4.7 Conductivity of CAB before and after emptying trap levels

	Conductivity,σ x 10^{-11} /Scm^{-1}	
	Before Empty Trap	After Empty Trap
Forward	4.2 ± 0.3	4.26 ± 0.02
Reverse	4.64 ± 0.03	4.06 ± 0.04

The conduction mechanism for CAB is by intrachain and interchain hopping. The intrachain hopping results from sigma (σ) orbital overlap while the interchain hopping results from pi (π) orbital overlap. Even though σ overlap is less efficient than π overlap, the higher potential energy of interchain hopping is the limiting factor in the conductivity of CAB.

CAB is expected to have higher conductivity than CB at room temperature because the presence of electron donating $-NH_2$ group at the benzoate ligand is expected to increase the electron density in the ring and to reduce the interchain distance through the formation of hydrogen bonding.

The $-NH_2$ group at the benzoate ligand is responsible for the resonance as shown in Figure 4.5. This results in partial positive charge on nitrogen atom which

inhibit the formation of hydrogen bonding between chains and increase interchain distance due to repulsion. The increase interchain distance that resulted should reduce the interchain conduction. It was reported that in a group of isonitrile derivatives of the type $[Pt(CNR)_4]$ $[PtCl_4]$ with R as aryl groups, electron-donating substituents on the ligand weaken the metal-metal interaction in the chain [6], thus reducing the intrachain conduction. These two factors may explain why the conductivity of CAB is not higher than CB as expected.

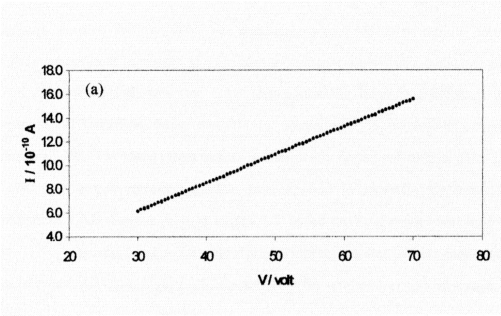

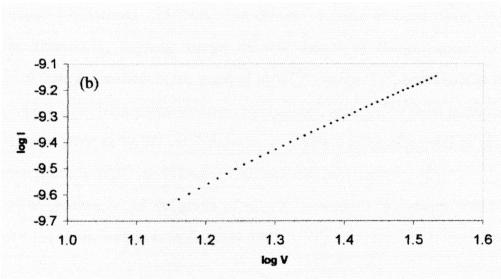

Figure 4.9 Graph of (a) I vs V and (b) log I vs log V for copper(II) 4–aminobenzoate

Figure 4.10 shows the variation of conductivity of CAB as a function of temperature between 78K to 300K. The conductivity of CAB drops rapidly between 78-80K as temperature increases. It continues to decrease slowly at a constant rate up to 276K. This trend indicates that CAB shows metallic behaviour between those temperature. A transition from metallic to semiconductor behaviour occurs at temperature 276K. The same effect occurs in chemically doped polyaniline films [7].

Various carrier transport models were applied to ascertain the conducting mechanism of CAB. Graphs of ln σ versus 1/T based on band model and ln $[\sigma T^{1/2}]$ versus $T^{-1/4}$ based on Mott's Variable Range Hopping model (VRH) plotted were shown in Figure 4.11 and Figure 4.12 respectively for temperatures in the range 80K to 300K.

The graph of ln $(\sigma T^{1/2})$ versus $T^{-1/4}$ (Figure 4.12) indicates that CAB follows VRH model [8] between 276-300K. The density of states at Fermi level, $N(E_F)$; hopping distance, R; hopping energy, ΔE and density of charge carriers, n are calculated from the gradient of the graph of ln $(\sigma T^{1/2})$ versus $T^{-1/4}$ between 276-300K (Figure 4.13). The electron wave function localization length, α^{-1} is equal to the width of CAB unit, taken as $6x10^{-8}$ cm. The value is assumed to be twice that of pyrrole monomer which is $3x10^{-8}$ cm [9], since CAB unit may be a dimer.

The gradient, m of the graph of ln $(\sigma T^{1/2})$ versus $T^{-1/4}$ between 276-300K (Figure 4.13) can be written as in Equation 4.6.

$$m = -T_0^{1/4} = -\left(\frac{18.1\alpha^3}{kN(E_F)}\right)^{1/4} = -13.84K^{\frac{1}{4}} \qquad 4.6$$

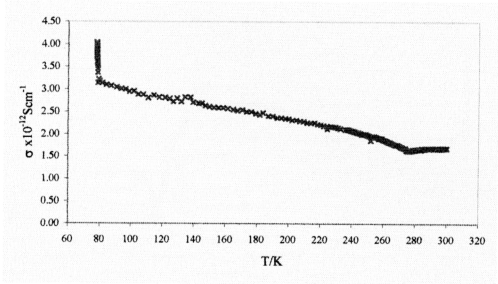

Figure 4.10 Graph of conductivity, σ vs. temperature, T of copper(II) 4–aminobenzoate

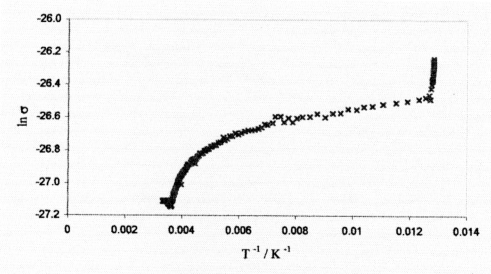

Figure 4.11 Graph of ln σ vs T^{-1} of copper(II) 4-aminobenzoate

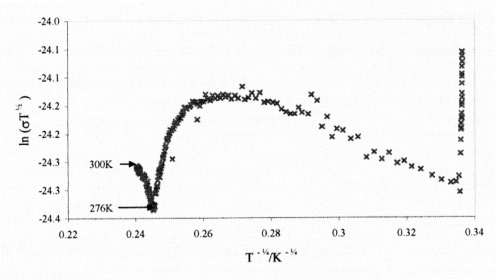

Figure 4.12 Graph of ln ($\sigma T^{1/2}$) vs $T^{-1/4}$ of copper(II) 4-aminobenzoate

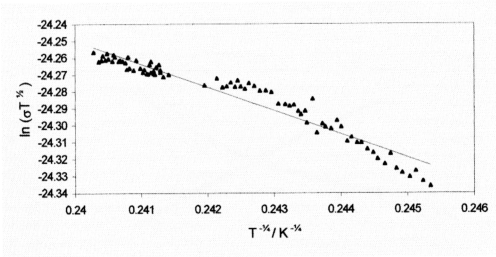

Figure 4.13 Graph of ln ($\sigma T^{1/2}$) vs $T^{-1/4}$ of copper(II) 4-aminobenzoate for temperature range 276K-300K

The density of states at Fermi level, $N(E_F)$ for CAB was calculated using Equation 4.6. The relationship between R, ΔE and n with temperature are given by Equations 2.5, 2.6 and 2.7 and rewritten as Equations 4.7, 4.8 and 4.9 and tabulated in Table 4.8 for T=300K. The variation of R, ΔE and n respectively with temperature are shown graphically in Figure 4.14 and 4.15.

$$R = 3.11 \times 10^{-7}\, T^{-1/4}\ \text{cm} \qquad 4.7$$

$$\Delta E = 2.98 \times 10^{-4}\, T^{3/4}\ \text{eV} \qquad 4.8$$

$$n = 2.29 \times 10^{18} T\ \text{cm}^{-3} \qquad 4.9$$

Table 4.8 Mott's variable range hopping parameter for CAB

Gradient of graph, m	-13.8 $K^{1/4}$
Density of states at Fermi level, $N(E_F)$	2.65×10^{22} $(eV)^{-1}cm^{-3}$
Hopping distance, R	7.47×10^{-8} cm (300K)
Hopping energy, ΔE	0.02 eV (300K)
Density of charge carriers, n	6.87×10^{20} cm^{-3} (300K)

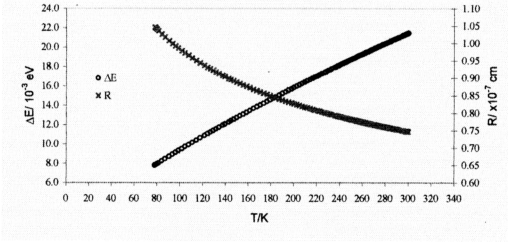

Figure 4.14 Graph of hopping distance, R and hopping energy, ΔE vs temperature, T for CAB

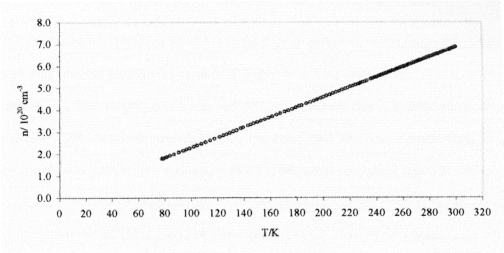

Figure 4.15 Graph of density of charge carriers, n vs temperature, T for CAB

The density of states, hopping distance and hopping energy at 300K for CAB are $2.29x10^{18}$ $(eV)^{-1}cm^{-3}$, $7.47x10^{-8}$ cm and 0.02 eV respectively. These values may be compared to that of polypyrrole films at 10^{18}-10^{22} $(eV)^{-1}cm^{-3}$, $5.81x10^{-8}$ cm and 0.08 eV respectively at the same temperature [9].

4.2.2 Conductivity of Copper(II) 4–Aminobenzoate Doped with Iodine

The conductivity data of CAB doped with different percentage of iodine for forward and reverse polarity is shown in Table 4.9. The graphs are plotted in Figures 4.16 and 4.17 respectively. It is observed that the conductivity is almost constant up to 12% iodine. The conductivity started to increase and reached a maximum at 20% iodine and then decrease to a minimum at 24% before it increased again at 28%.

It may be concluded that iodine at concentration lower than 12% has no effect on the conductivity of CAB because the concentration of I_3^- or I_5^- counterions formed were not high enough to neutralise the partial charge on nitrogen atom in CAB. The partial charge on the nitrogen was fully neutralised at 20% iodine. Between 20%-24% iodine, the conductivity decreased to a minimum because the incorporation of additional iodine molecules may disturb the carrier transport, as suggested for DA complex [10]. After 24%, the increase in conductivity cannot yet be explain until further studies are done.

Table 4.9 Conductivity of CAB doped with different amounts of iodine before and after emptying trap levels

Percentage of Iodine / %	Conductivity, $\sigma \times 10^{-11}$ / Scm^{-1}			
	Forward		Reverse	
	Before Empty Trap	After Empty Trap	Before Empty Trap	After Empty Trap
0.0	4.2 ± 0.3	4.26 ± 0.02	4.64 ± 0.03	4.06 ± 0.04
4.0	3.0 ± 0.2	2.8 ± 0.1	2.69 ± 0.06	2.95 ± 0.04
7.9	4.1 ± 0.4	3.68 ± 0.03	3.4 ± 0.1	3.76 ± 0.02
12.0	3.4 ± 0.3	2.78 ± 0.05	2.92 ± 0.08	2.79 ± 0.03
16.0	33 ± 3	24.7 ± 0.2	28.7 ± 0.6	24.2 ± 0.1
20.0	54 ± 4	25.3 ± 0.1	34 ± 5	40 ± 10
23.9	14 ± 2	0.92 ± 0.02	10.4 ± 0.3	1.1 ± 0.2
27.9	35 ± 3	27.1 ± 0.2	30.6 ± 0.9	26.89 ± 0.06

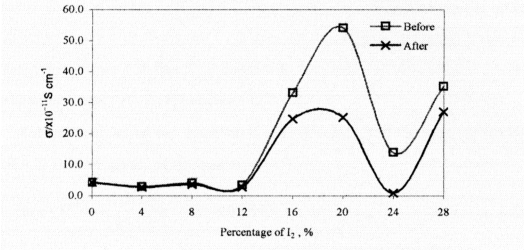

Figure 4.16 Graph of conductivity, σ vs percentage of iodine in forward polarity

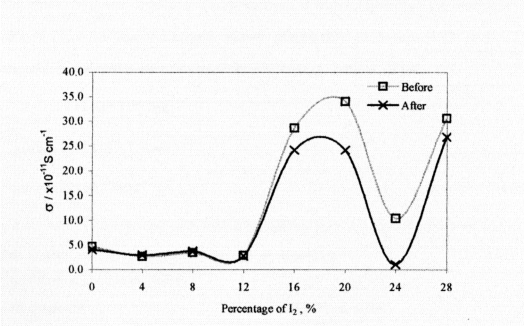

Figure 4.17 Graph of conductivity, σ vs percentage of iodine in reverse polarity

Figure 4.18 shows the conductivity versus temperature for CAB doped with 20% iodine. The graph shows that the sample exhibit metallic behaviour from 80-300K. Band and Mott's transport models were applied to the material and the resultant graphs are shown in Figure 4.19 and 4.20 respectively for temperatures in the range 80K to 300K. Figure 4.19 shows that CAB does not follow the band model. It may be concluded from Figure 4.20 that CAB doped with 20% iodine follows Mott's variable range hopping model (VRH) [8] between 147-300K.

The gradient, m of the graph of $\ln(\sigma T^{1/2})$ versus $T^{-1/4}$ between 147-300K (Figure 4.21) can be written as in Equation 4.10.

$$m = -T_o^{1/4} = -\left(\frac{18.1\alpha^3}{kN(E_F)}\right)^{1/4} = -8.05\,K^{1/4} \qquad 4.10$$

The density of states at Fermi level, $N(E_F)$ was calculated using Equation 4.10. From Equation 2.5, 2.6 and 2.7, the relationship between hopping distance, R; hopping energy, ΔE and density of charge carriers, n with temperature are rewritten in Equation 4.11, 4.12 and 4.13, and shown graphically in Figure 4.22 and 4.23 respectively. R, ΔE and n are calculated for T=300K in Table 4.10 [8].

$$R = 3.11\times10^{-7}\,T^{-1/4}\ cm \qquad 4.11$$

$$\Delta E = 2.98\times10^{-4}\,T^{3/4}\ eV \qquad 4.12$$

$$n = 2.29\times10^{18}\,T\ cm^{-3} \qquad 4.13$$

Table 4.10 Mott's variable range hopping parameter for CAB doped with 20% iodine

Gradient of graph, m	$-8.05425\ K^{1/4}$
Density of states at Fermi level, $N(E_F)$	$2.31\times10^{23}\ (eV)^{-1}cm^{-3}$
Hopping distance, R	4.35×10^{-8} cm (300K)
Hopping energy, ΔE	0.013 eV (300K)
Density of charge carriers, n	$5.97\times10^{21}\ cm^{-3}$ (300K)

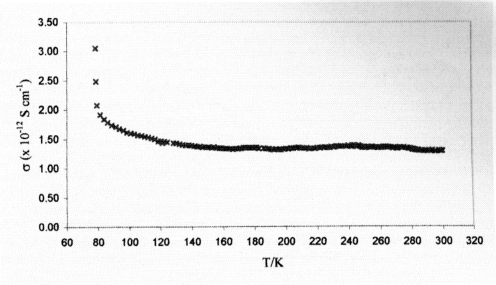

Figure 4.18 Graph of conductivity, σ vs. temperature, T for CAB doped with 20% iodine

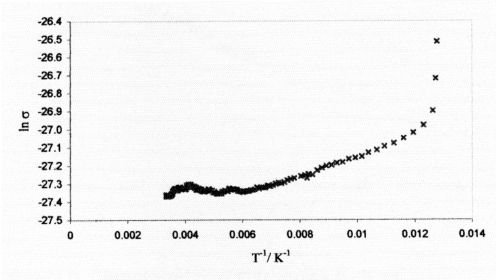

Figure 4.19 Graph of ln σ vs T^{-1} for CAB doped with 20% iodine

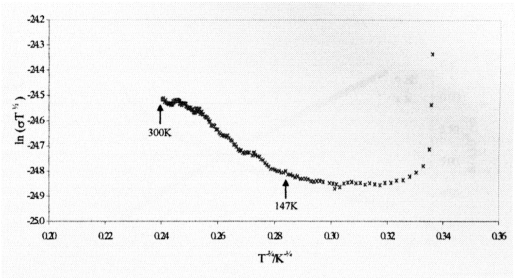

Figure 4.20 Graph of ln ($\sigma T^{1/2}$) vs $T^{-1/4}$ CAB doped with 20% iodine

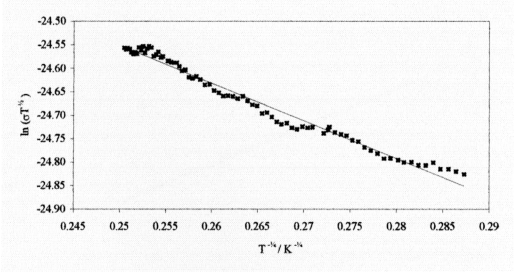

Figure 4.21 Graph of ln ($\sigma T^{1/2}$) vs $T^{-1/4}$ CAB doped with 20% iodine for temperature range 147-300K

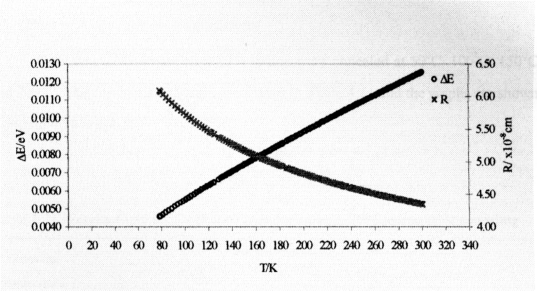

Figure 4.22 Graph of hopping distance, R and hopping energy, ΔE vs temperature, T for CAB doped with 20% iodine

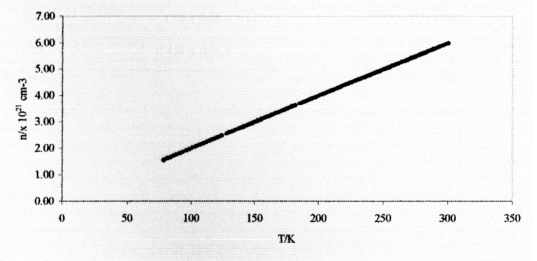

Figure 4.23 Graph of density of charge carriers, n vs temperature, T for CAB doped with 20% iodine

4.3 Effect of Annealing on Conductivity

CAB and CAB doped with 20% iodine were annealed at 50^0C, 100^0C, 150^0C and 200^0C. The conductivity values are shown in Table 4.11 and the graphs are shown in Figure 4.24 and 4.25.

Table 4.11 Conductivity for CAB and CAB doped with 20% iodine after annealing

Annealing temperature / ^{0}C	Conductivity,σ x 10^{-10} / Scm^{-1}	
	CAB	20% iodine-doped CAB
	After Empty Trap	After Empty Trap
unannealed	0.426 ± 0.003	2.52 ± 0.01
50	0.391 ± 0.003	1.52 ± 0.07
100	2.7 ± 0.1	1.13 ± 0.02
150	4.56 ± 0.06	1.47 ± 0.01
200	0.454 ± 0.002	2.24 ± 0.01

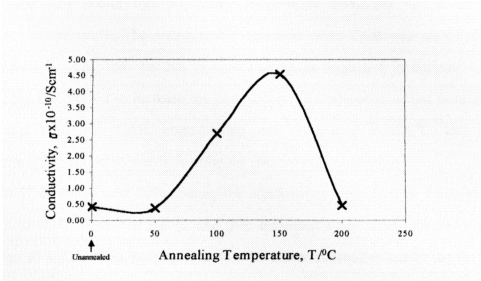

Figure 4.24 Graph of conductivity, σ vs annealing temperature, T for CAB

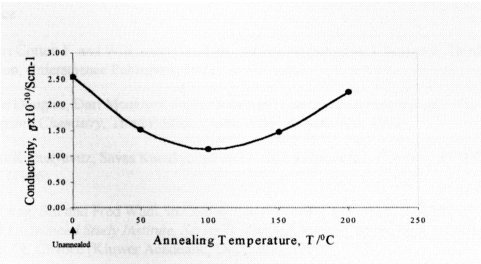

Figure 4.25 Graph of conductivity, σ vs annealing temperature, T for CAB doped with 20% iodine

Figure 4.24 shows that annealing of CAB at 50°C did not affect its conductivity significantly. The conductivity increased when CAB was annealed at 100°C and 150°C. This may be due to cross-linking as suggested in Section 4.13. Cross-linking is expected to increase the conductivity if conjugation is not destroyed at the same time. For CAB, cross-linking was completed at 200°C, and the conductivity decreased to its previous value for reasons not yet obvious.

For CAB doped with 20% iodine, the conductivity decreased to a minimum value of 1.13×10^{-10} Scm^{-1} at 100°C, and then increased again. This may be due to sublimation of iodine upon heating. The loss of iodine molecules cause the carrier concentration to reduce and hopping distance to increase. At annealing temperatures of 150°C and 200°C, the trend in conductivity was similar to that of CAB, and may be due to the same reasons.

Reference

1. Albert Cotton F. and Wilkinson Geoffrey, *Advanced Inorganic Chemistry,* Third Edition, (Interscience Publishers, 1972)

2. Bodie Douglas, Darl Mcdaniel, John Alexander, *Concepts and Models of Inorganic Chemistry,* Third Edition, (John Wiley & Sons, Inc, 1993)

3. Zuhal Kucukyavuz, Savas Kucukyavuz and Nahid Abbasnejad, *Polymer,* **37 (15),** 3215 (1996)

4. Songqing, Shi and Fred Wudl, in *Conjugated Polymeric Materials,* Vol.182 of *NATO Advanced Study Institute, Series E: Applied Science,* edited by J. L.Bredas and R. R. Chance (Kluwer Academic, Dopdrecht, 1990)

5. Unpublished Results

6. H. J. Keller in *Low Dimensional Cooperative Phenomena* edited by H. J. Keller, (Plenum Press, New York and London, 1975)

7. A. N. Aleshin, N. B. Mironkov, A.V. Suvorov, J. A. Conklin, T. M. Su and R. B. Kaner, *Physical Review B,* **54, (16),** 11638, (1996)

8. Brodsky M. H., Carlson D., Cornell G. A. N., Davis E. A., Fischer R., Hayes T. M. Kramer B., LeComber P. G., Lucovsky G., Nagels P., Solomon I., Spear W. E., Weaire D. L., Wronski C. R. *Amorphous Semiconductor*, (Springer-Verlag Berlin Heidelberg, 1979)

9. Maddison D. S. and Tansley T. L., *J. Appl. Phys.*, **72** (10), (1992)

10. Hans Meier in *Organic Semiconductors*, Vol.2 of *Monograph in Modern Chemistry*, edited by Hans F. Edel (Verlag Chemie, 1974)

11. W. Eevers, M. De Wit, J. Briers, R. Mertens, P. Nagels, R. Callaerts, W. Herrebout and Van der Veken, *Polymer*, **35**, 4573, (1994)